Materials Sciences and Applications, 2024, 15, 168-185
https://www.scirp.org/journal/msa
ISSN Online: 2153-1188
ISSN Print: 2153-117X

Removal of Dyes in Aqueous Media with Hydrochar Base of Solid Tanneries Waste: Optimization Process and Application

Abdoul Ntieche Rahman[1*], Gervais Ndongo Kounou[2], Sakué Ngankam Eric[2], Tamafo Fouegue Aymard Didier[1], Kouotou Daouda[2], Abdelaziz Baçaoui[3]

[1]Department of Chemistry, Higher Teacher Training College Bertoua, The University of Bertoua, Bertoua, Cameroon
[2]Department of Fundamental Sciences, Institute of Wood Technology of Mbalmayo, University of Yaoundé I, Balmayo, Cameroon
[3]Department of Chemistry, Faculty of Science Semlalia, University of Cady Ayyad, Marrakech, Morocco
Email: *rahmino@gmail.com

How to cite this paper: Rahman, A.N., Kounou, G.N., Eric, S.N., Didier, T.F.A., Daouda, K. and Baçaoui, A. (2024) Removal of Dyes in Aqueous Media with Hydrochar Base of Solid Tanneries Waste: Optimization Process and Application. *Materials Sciences and Applications*, **15**, 168-185.
https://doi.org/10.4236/msa.2024.157012

Received: May 23, 2024
Accepted: July 8, 2024
Published: July 11, 2024

Abstract

The Response Surface Methodology (RSM) was used to optimise the conditions of preparation of activated hydrochar from tannery solid waste by hydrothermal carbonisation (HTC). The main factors such as residence time, moisture content and final carbonisation temperature were investigated during the optimisation of hydrochar preparation conditions. The three responses investigated are hydrochar yield, iodine and methylene blue indices. The results of experimental analyses showed that the yield of hydrochar decreases with increasing final temperature, leading to the formation of micropores inside the carbonaceous solid. The optimum conditions for preparing the following hydrochar were obtained: 83.10%, 390.44 $mg{\cdot}g^{-1}$ and 259.63 $mg{\cdot}g^{-1}$ respectively for the hydrochar yield, the iodine and methylene blue indices. The specific surface area of prepared hydrochar is 849.160 m^2/g, SEM micrographs showed a porous heterogeneous surface and particularly, the hydrochar surface also revealed external pores on the hydrochar surface which acted as a pathway to the micropores. Fourier transform infrared (FTIR), however, showed a predominance of acid functions on the surface of the carbonaceous solids. Tests were carried out to eliminate indigo carmine in aqueous media. Activated hydrochar showed a high level of activity, with the Langmuir and Freundlich isotherms giving an adsorption quantity of 354.610 mol/g and a K_F constant of 468.2489, respectively. The findings of the research revealed that hydrochar produced is well adapted for dyes removal.

Keywords

Response Surface Methodology, Hydrochar, Tannery, Hydrothermal

Carbonization, Adsorption

1. Introduction

Today, the world is experiencing rapid demographic expansion and rising living standards. This challenge must be met and the solution must take into account new resources, such as new energies and diverse natural resources, appropriate to their abundance and availability [1] [2]. The use of biomass appears to be an essential solution to all these problems. In order to be useful, biomass needs to be processed in a way that respects energy standards and environmental balance. Carbonaceous materials derived from biomass waste have shown suitable applications for sorption utilities. They have a high adsorption capacity, are effective at adsorbing substances in low concentrations and are highly selective. In addition to their easy regeneration and their low production cost, these criteria required for their use as adsorbents. However, the problem remains that there is as yet no suitable process for producing valuable carbonaceous materials from raw biomass waste [3]-[6]. From this perspective, the hydrothermal carbonisation (HTC) process could be the economic cornerstone and a promising method to exploit. The HTC process offers a number of advantages, many organic wastes are found in aqueous media and obviously have a high water content, which makes the HTC process perfectly adapted to the carbonisation of these materials; no drying process is required, the HTC method saves 50% energy compared with other methods that require prior drying [7]-[12]. It also allows the inorganic elemental compositions to be washed out of the liquid phase and considerably reduces the ash content. Solid waste from tanneries is found everywhere in the environment, mainly in very humid aqueous environment [13]-[16]. The tanning industries discharge huge quantities of solid waste (mainly hair, flesh fragments and hides from slaughtered animals such as sheep, goats and cows) and wastewater (sodium and ammonium salts, acids, lime, chlorides, surfactants, chromium (III and 7) and dyes into the environment. The environmental effects of the tanning process are significant and must be taken into consideration despite the socio-economic impact of the tanning industries through job creation and income generation [17]-[21].

The main objective of this paper is to solve the problem of pollution caused by tannery waste by directly converting vegetable-tanned shaved leather (VTS) into carbonaceous adsorbents: using the HTC method [21]. The hydrochar was used for removal dyes on liquid waste from tanneries. To achieve this goal, optimization through the response surface methodology involving screening of parameters has been adopted. Owing to the fact that the hydrochar material prepared will be used for decoloration of water, domains of variation of predictive variables such as hydrochar yield, Yld (%); iodine number, ION ($mg{\cdot}g^{-1}$); and methylene blue number, MBN ($mg{\cdot}g^{-1}$) will be studied in order to obtain the hy-

drochar characteristics required.

2. Experimental Method

2.1. Hydrothermal Carbonization Process of Biomass

The method for preparing hydrochar was described in our previous work. As a matter of fact the vegetable-tanned leather shavings (VTS) used in this study were collected from a traditional tannery in Marrakech, Morocco. An exact amount of 15.5 mg of VTS with different moisture contents were loaded into a reactor associated with an autoclave that was heated from room temperature (18˚C) up to the target temperature set under an N_2 atmosphere at the heating rate of 5˚C·min^{-1}. At each final temperature and residence time, the oven was turned off and allowed to cool to room temperature inside the autoclave. The resulting hydrochar was labelled as VTS-HTC and was weighed following equation (1). The VTS-HTC was then oven-dried at 105˚C for 24 h.

$$\text{VTS-HTC mass yeild}(\%) = \frac{m_{\text{hydochar}}}{\text{masse}_{\text{VTS}}} \times 100 \tag{1}$$

m_{hydochar} in Equation (1) is the mass of the hydrochar after being dried and mass_{VTS} is the mass of the raw material with moisture. After the hydrocarbonization process, about 5.0 to 6.0 g of the hydrochar was subjected to physical activation with steam (0.13 ml·min^{-1}) in a furnace by heating the reactor from room temperature up to 850˚C at the heating rate of 10˚C·min^{-1} for 2 h of residence time.

2.2. Optimization Process

The hydrothermal carbonization process parameters were studied using the response surface methodology (RSM) (**Figure 1**). The RSM is a statistical technique that is useful for modelling and analysing problems where a response of interest is influenced by several variables. RSM aims at reducing the number of experiments to be performed, while simultaneously studying the effects of several factors, as well as helping to analyse interactions between the parameters studied [22] [23].

The most influential experimental factors on the final characteristics of carbonaceous material obtained from HTC are the carbonization temperature (X_1), the residence time (X_2) and the moisture content (X_3). The three responses analysed were hydrochar yield (Y_1), iodine number, (Y_2) and methylene blue number (Y_3). The Doehlert's experimental matrix and the corresponding experimental conditions of the responses Y_1, Y_2 and Y_3 are given in **Table 1**. Each response was used to develop a model correlating the responses to the three coded factors using a polynomial equation as follows:

$$\begin{aligned} Y_i = {} & b_0 + b_1X_1 + b_2X_2 + b_3X_3 + b_{11}X_{21} + b_{22}X_{22} + b_{33}X_{23} \\ & + b_{12}X_1X_2 + b_{13}X_1X_3 + b_{23}X_2X_3 + \text{residual} \end{aligned} \tag{2}$$

Table 1. Doehlert's experimental matrix, the corresponding experimental conditions and responses.

N˚ Exp	Rand	Temperature (X_1)	Residence time (X_2)	Humidity content (X_3)	Y_1	Y_2	Y_3
1	1	290	75	70.0	55.00	279.19	240.00
2	2	190	75	70.0	85.00	301.39	260.00
3	3	265	110	70.0	57.00	260.00	50.00
4	4	215	40	70.0	75.00	210.00	96.00
5	5	265	40	70.0	60.00	317.00	180.00
6	6	215	110	70.0	72.00	412.00	120.00
7	7	265	87	78.2	55.17	222.03	110.00
8	8	215	63	61.8	78.00	307.26	200.00
9	9	265	63	61.8	61.40	285.50	230.00
10	10	240	98	61.8	68.00	348.99	180.00
11	11	215	87	78.2	73.86	253.81	140.00
12	12	240	52	78.2	65.00	257.00	198.00
13	13	240	75	70.0	66.00	252.26	60.00
14	14	240	75	70.0	64.73	269.67	80.00
15	15	240	75	70.0	65.60	226.78	80.00
16	16	240	75	70.0	65.00	279.19	70.00
17	17	240	75	70.0	67.00	317.26	95.00

Y_1: yeild (%); Y_2: iodine number (mg/g); Y_3: methylene blue number méthylène (mg/g).

In Equation (2.2), Y_i is the predicted response, b_0 is a constant coefficient, b_i is a linear coefficient; b_{ii} is a quadratic coefficient, b_{ij} is an interaction coefficient; X_1, X_2 and X_3, are the coded values of the respective factors.

2.3. Carbonaceous Material Characterization

The activated hydrochar obtained at the optimal condition was characterized by various physicochemical methods. The hydrochar adsorptive property in liquid phase was determined by iodine and methylene blue adsorption capacities. The textural characteristics of the activated hydrochar were obtained using a chemisorption and physisorption surface area analyser (Micromeritics TriStar 3000). The surface functional groups of the obtained samples were determined by Fourier transform infrared (FTIR) spectrum using FT-IRSPECTRUM ONE brand, the wave number was found between 450 and 4000 cm^{-1}. The surface morphology was investigated using scanning electron microscopy (SEM) (VEGA3 TESCAN). Elemental energy dispersive X-ray (EDX) analysis was done using EDAX TEAM, 125.9 eV of resolution and was applied to investigate the presence and percentage of atoms that made up the AH.

2.4. Adsorption of Indigo Carmine

Indigo carmine is a member of the indigoid family, a blue dye used to colour textiles, particularly jeans. Because of their toxicity and reactivity, the presence of dyes in the environment has given rise to considerable concern. The performance of the prepared activated hydrochar was evaluated on the removal of indigoid dye in aqueous solution.

The adsorption equilibrium of indigo carmine studies was performed using isotherm technique. 600 mg of IC is weighed and introduced in a 2 litres volumetric flask. The flask is then filled with distilled water up to the calibrated mark. The solution is left under stirring for 12 hours and is then filtered to eliminate undissolved particles. A volume V of the parent solution is taken, put in a 100 mL volumetric flask and completed with distilled water to the calibrated mark. 50 mL of solution so obtained is put in a bottle containing 10 mg of activated carbon and shaken vigorously using a magnetic stirrer at the rate of 200 r.p.m. at room temperature for 4.0 h. Eight solutions of different concentrations are thus prepared by varying the volume V of the parent solution from 2.5 to 20 mL. At the end of the adsorption process, the solutions were filtered and the equilibrium concentrations were determined by spectrophotometric analysis.

The quantities of micropollutants adsorbed are calculated using the following equation:

$$Q_{ads} = \frac{(C_0 - C_e)V}{m} \tag{3}$$

where Q_{ads} is the quantity of dye adsorbed per unit mass of Hydrochar (in $mg{\cdot}g^{-1}$), C_0 and C_e are respectively the initial concentration and equilibrium concentration of the coloured solution respectively; V the volume (L), and m is the weight (g) of the adsorbent.

The linear and non-linear equations of isotherms and kinetics models with the respective error functions are compiled in Table 2.

Table 2. Nonlinear and linear equations of isotherm and kinetic models and errors functions.

Models	Nonlinear equations	Linear equations
	Isotherms models	
Langmuir	$Q_e = \frac{Q_m K_L C_e}{1 + K_L C_e}$	$\frac{C_e}{Q_e} = \frac{1}{Q_m K_L} + \frac{C_e}{Q_m}$
Freundlich	$Q_e = K_F C_e^{1/n}$	$\ln Q_e = \ln K_F + \frac{1}{n}\ln C_e$
Tempkin	$Q_e = \frac{RT}{b}\ln(K_T C_e)$	$Q_e = \frac{RT}{b}\ln K_T + \frac{RT}{b}\ln C_e$
DKR	$Q_e = q_s \exp\left(-k_{ad}\left[RT\ln\left(1+\frac{1}{C_e}\right)\right]^2\right)$	$\ln Q_e = \ln Q_m - K_{ad}\left[RT\ln\left(1+\frac{1}{C_e}\right)\right]^2$

3. Results and Discussions

3.1. Response Surface Analysis

The responses selected in this work are useful tools to provide important information on indigo carmine removal by the activated Hydrochar. The hydrochar yield (Y_1) studied here as the percentage of weight loss is useful to predict the porous structure of the prepared Hydrochar. The iodine adsorption test (Y_2) indicates the microporosity of carbon material it translates the affinity of adsorption of material for small molecules and finally the methylene blue (Y_3) has an average size representative model of organic pollutants which is used to evaluate the performance of carbon before its use in water treatment, bleaching of vegetable oils and other uses [22].

Thus, the resulting polynomial models from these analyses are represented by the following equations.

$$Y_1 = 65.420 - 15.399X_1 - 1.622X_2 - 3.056X_3 + 4.574X_1^2 - 0.593X_2^2 + 1.623X_3^2 + 0.289X_1X_2 - 2.362X_1X_3 - 0.402X_2X_3 \quad (4)$$

$$Y_2 = 78.200 - 3.750X_1 - 36.807X_2 - 36.742X_3 + 171.800X_1^2 - 14.868X_2^2 - 103.467X_3^2 - 92.379X_1X_2 - 4.079X_1X_3 - 80.133X_2X_3 \quad (5)$$

$$Y_3 = 254.322 - 16.611X_1 + 38.401X_2 - 42.633X_3 + 35.968X_1^2 + 48.584X_2^2 + 29.037X_3^2 - 149.538X_1X_2 + 52.892X_1X_3 - 49.742X_2X_3 \quad (6)$$

By simply solving the equation through the regression method based on the least squares optimisation criterion, the values of the coefficients (**Table 3**) of the regression are directly obtained using the NEMROD (New Efficient Methodology of research using optimal design) software.

Table 3. Estimated values of coefficients for Hydrochar yield (Y_1), iodine number (Y_2) and methylene blue number (Y_3).

Name	Coefficient	Signif	Coefficient	Signif	Coefficient	Signif
	Hydrochar yield (Y_1)		Iodine (Y_2)		Methylene blue (Y_3)	
b_0	65.43	<0.01***	78.20	<0.01***	254.32	<0.01***
b_1	−15.40	<0.01***	−3.75	45.6	−16.61	0.217**
b_2	−1.62	0.381**	−36.81	0.016***	38.40	<0.01***
b_3	−3.06	0.014***	−36.74	0.017***	−42.63	<0.01***
b_{11}	4.57	0.025***	171.80	<0.01***	35.97	0.056***
b_{22}	−0.59		−14.87	9.9	48.58	0.012***
b_{33}	1.62	2.86	103.47	<.001***	21.04	0.634**
b_{12}	0.29	74.8	−92.38	0.01***	−149.5	<0.01***
b_{13}	−2.36	4.51*	−4.08	74.4	52.89	0.073***
b_{23}	−0.40	69.3	−80.13	0.04***	−49.74	0.100**

*** most significant effect, ** less significant effect, * no significant effect.

From Equation (4), we notice that only temperature has the largest influence on the response Y_1, the hydrochar yield. The effect of temperature is negative ($b_1 < 0$) on hydrochar yield, indicating that the hydrochar yield rapidly decreases (about 15.4%) with increasing hydro carbonisation temperature. This happens because of the departure of volatile inside the precursor. This trend has been observed by other authors [22]-[29]. The regression coefficient measured the degree of fitness of the model, $R^2 = 0.996$, indicating that 99.6% of the total variation in the hydrochar yield was explained by the fitted model. In addition, the R^2-ajusted coefficient ($R_A^2 = 0.991$) is also high and close to R^2, confirming that the generated models are accurate [30].

All the coefficients except the quadratique coefficient of the carbonization temperature from the regression equation describing the iodine number (Y_2) are negative. This shows their antagonist effects on the production of micropores into the hydrochar structure. Furthermore, the quadratic term coefficients related to temperature is positive and higher, indicating a particular impact of the temperature on the micropore volume obtained. A slow rate of temperature rise facilitates the release of volatile compounds by keeping the structure of the hydrochar identical to the structure of the raw material and leading to the formation of micropores. The correlation coefficient (R^2) and the R^2-ajusted of the response Y_2 are 0.991 and 0.980respectively, indicating a good agreement between the experimental and predicted values. Concerning the equation model of methylene blue (Y_3), the linear term coefficients related to the residence time is positive showing its significant effect on the MB adsorption. The interaction term coefficient ($|b_{12}| = 149.54$) shows that the combined effect between temperature and residence time of carbonization enhances the opening of the external pore and facilitates the formation of a network of pores into hydrocarbon.

According to the established model, **Figures 1~3** show the contour plots and response surface curves used to show the most important factors for hydrochar yield, iodine and methylene blue number respectively.

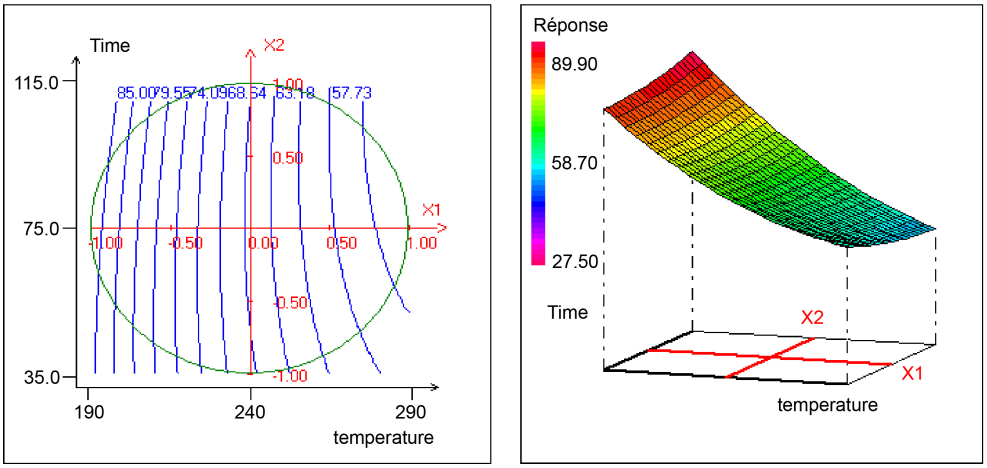

Figure 1. Surface plot and Contour plot of the variation of the hydrochar yield (Y_1) versus the temperature and time (X_1, X_2).

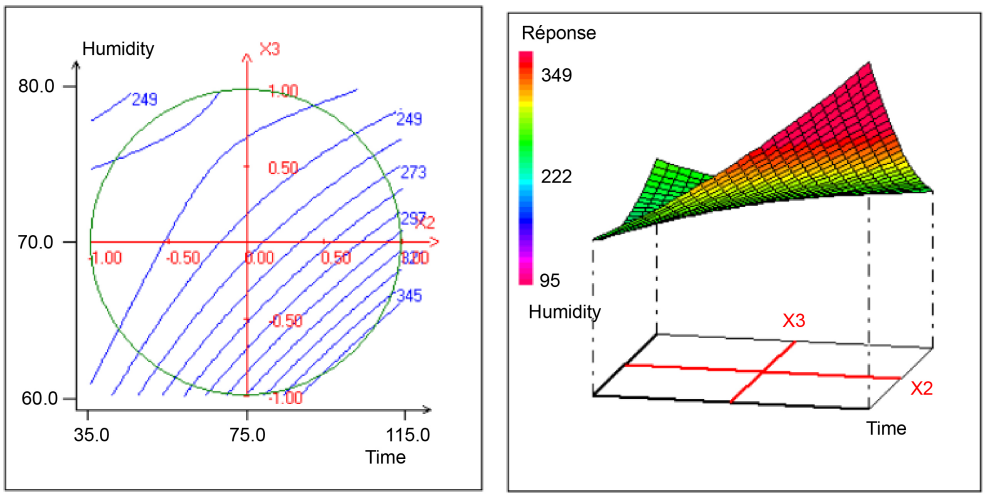

Figure 2. Surface plot and Contour plot of the variation of the iodine number (Y_2) versus the time and the humidity (X_2, X_3).

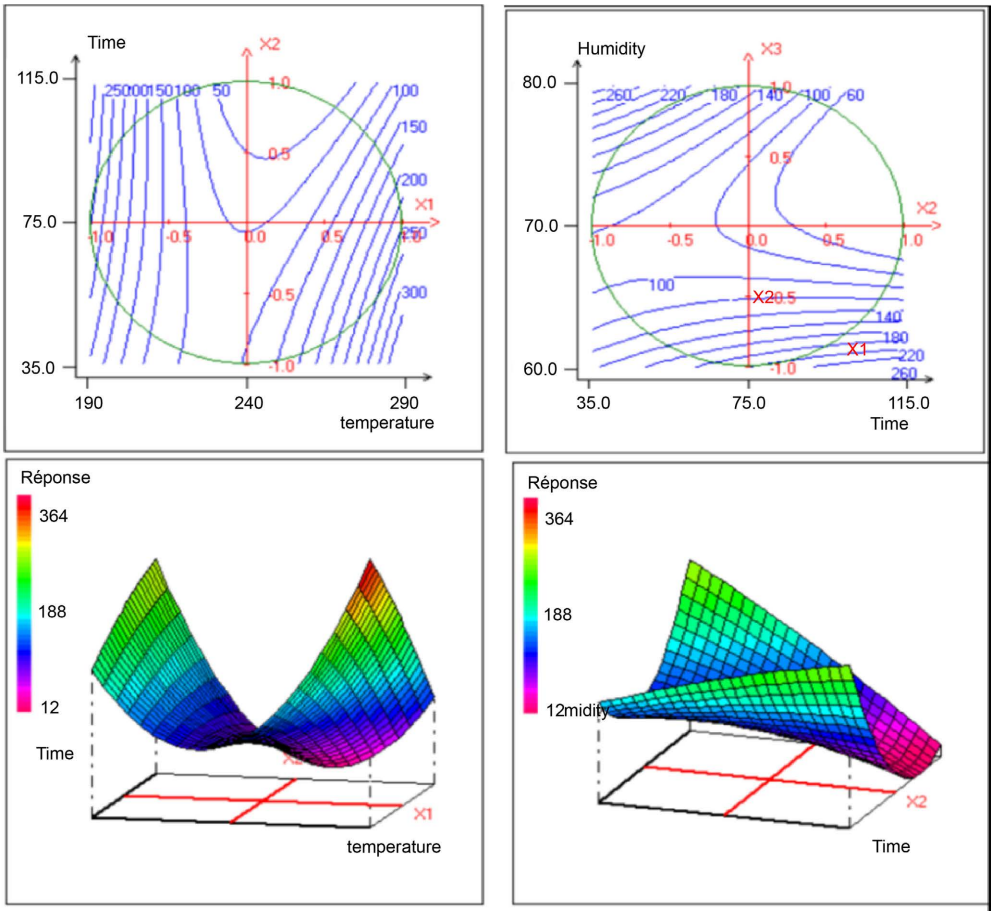

Figure 3. Surface plot and Contour plot of the variation of the methylene blue adsorption (Y_3) versus the temperature, residence time and humidity (X_1, X_2, X_3).

The analysis of the plot (Figure 1) shows that, with the increase in temperature (X_1) from 190˚C to 290˚C and the time (X_2) from 35 to 115 min, the hydrochar yield decreases from 85% to 57.73%. These two factors have a substan-

tial influence on the response (Y_1). This is because, as the temperature of hydro-carbonisation increases, there is a release of heteroatoms leading to an inevitable loss of mass. The HTC process involves three main reactions that are: dehydration, condensation and decarboxylation, resulting in a mass loss. As mentioned in Y_2 equation analysis, Figure 2 shows that the time (X_2) and the humidity (X_3) are the two main influencing factors. Indeed, the amount of iodine adsorbed decreases from 345 mg/g to 249 mg/ g with increasing in humidity. Since the iodine number gives an indication on the opened microporosity of the material, for the humidity less than the centre point, the increase in humidity facilitates micro pores formation. The variation of the methylene blue adsorption (Figure 3) shows that when the temperature increases from 190 to 290˚C, with the time from 35 to 115 min, the MBN increased from 100 mg/g to 300 mg/g. When the time increased from 35 min to 115 min with the humidity level of 60% to 80%, the MBN also decreased from 260 mg/g to 100 mg/g. These results lead us to conclude that the increase in temperature facilitates the opening of the pores on hydrochar, which interestingly increases the adsorption of MB. On the other hand, the increase of humidity is favorable for the formation of micropores as it has also been observed in the adsorption of iodine.

The desirability functions for each response are given in Figure 4.

3.2. Optimization Using Model Equation

The optimum characteristics of the hydrochar were recorded in Table 4. The graphs of the desirability functions (Figure 4) of the responses show different levels of constraints. The respective minimum and maximum values are: 75.00 to 90.00% for Y_1, 180.00 to 360.00 mg/g for Y_2 and 300.00 to 620.00 mg/g for Y_3. The predicted values are: 83.10% for the hydrochar yield, 390.44 mg/g for iodine number and 259.63 mg/g for the methylene blue number, which correspond to the degrees of satisfaction of 53.98%, 28.26% and 44.24%, for Y_1, Y_2, Y_3 respectively. The superposition of the surface curves of Y_1, Y_2 and Y_3 helps to identify the optimal zone with the best compromise of desirability. The minimum and

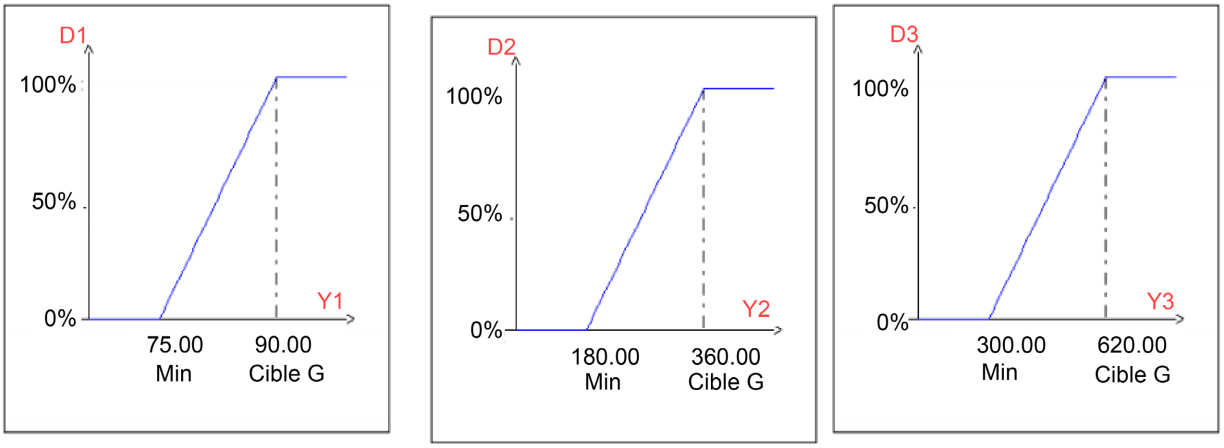

Figure 4. Graphs of the desirability functions for the responses Y_1, Y_2 and Y_3.

Table 4. Characteristics of hydro carbonization under optimum conditions.

Reposes	Name	Values	di %	Weights	di min %	di max %
Y_1	Yield	83.10	53.98	1	46.45	61.50
Y_2	ION	390.44	28.26	1	24.84	31.69
Y_3	MBN	259.63	44.24	1	35.67	52.81
	Desirability		40.72		34.53	46.86

Where di max % represents the degree of maximal satisfaction; di min %, the degree of minimal satisfaction and di% is the degree of satisfaction.

maximum values of the predicted desirability are from 34.53 to 45.86. The total desirability of the process is 40.72%, which is satisfactory since this value is within the predicted range. Figure 4 depicts the desired area of interest.

3.3. Characterization of Hydrochar Prepared under Optimum Condition

The SEM/EDX analysis (Figure 5) of the hydrochar obtained in the optimum condition was carried out using an apparatus of the JEOL JSM 6400 brand. It was found that the carbon material exhibits a polydisperse porous structure, made up of aggregates of different sizes and irregular shapes. The porosity is highly developed over the entire surface of the sample with certain heterogeneity due to the presence of three types of pores. Some white dots are observed from a close observation, attributable to the inorganic composition of precursor. The EDX analysis highlights the elements present on the surface of the hydrochar, consisting mainly of carbon (C) and calcium (Ca).

The FTIR spectrum (Figure 6) provides valuable information concerning the surface functional groups of the hydrochar material and might better help during its adsorption test. The hydrocarbon spectrum obtained at optimum conditions reveals the existence of several functional groups corresponding to characteristic bands. The adsorption band which appears at 3320 cm^{-1} can be

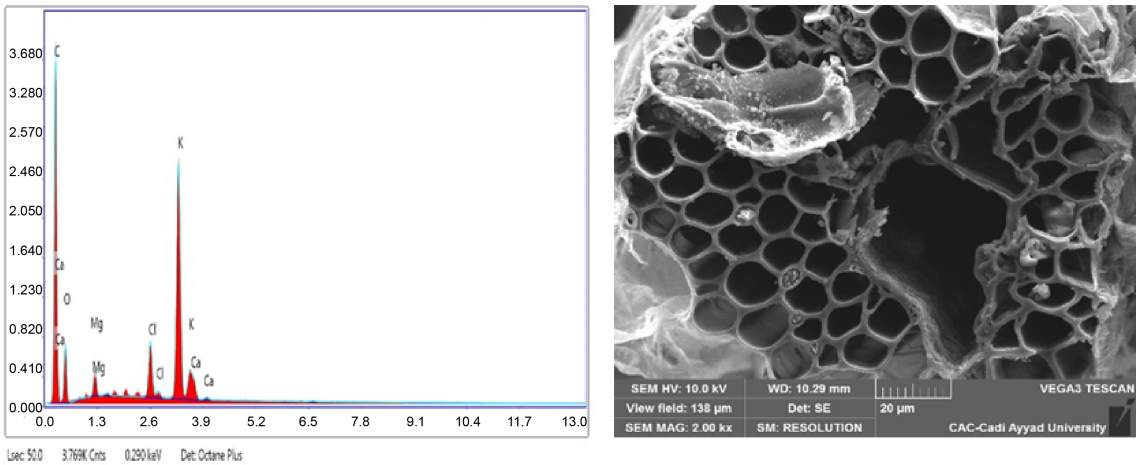

Figure 5. Scanning electron microscopy (SEM) of the sample of hydrochar obtained under optimum conditions.

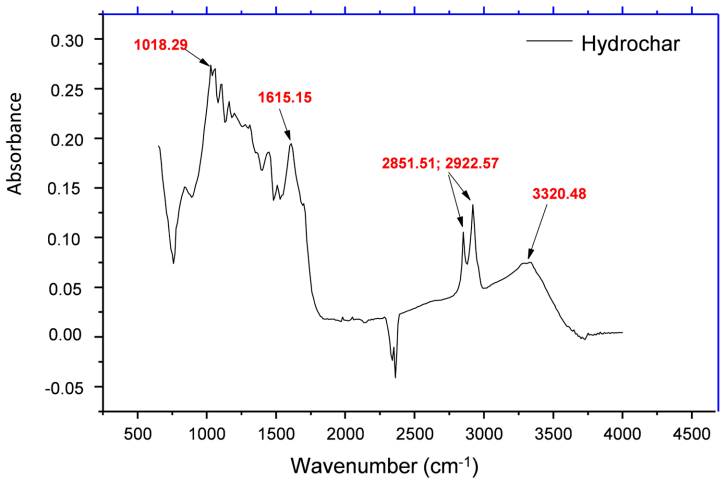

Figure 6. FTIR spectrum of *activated hydrochar* obtained under optimal conditions.

assigned to the OH stretching mode of hydroxyl groups, whereas the absorption band between 2851 and 2922 cm^{-1} corresponds to the C-H function [26]. The absorption peaks around 1615 and 1018 cm^{-1} can be attributed to C-N and C-O functions respectively.

Figure 7(a) shows a typical N_2 adsorption-desorption isotherm of the AH obtained from optimal condition. It exhibits the development of both micropores and mesopores. The sample presented greater adsorption capacities at low relative pressures P/Po < 0.1, indicating the presence of a more developed micropore structure; at relative pressure P/Po > 0.1 the filling of external pores by capillary condensation is observed. The isotherm of the AH sample is of type II with H_3 hysteresis according to the IUPAC, which is associated with a narrow pore size distribution of microporous material. The considerable intensity of hysteresis implies the presence of a network of interconnected pores that open onto the surface via external pores. This can be attributed to the physical activation of hydrochar by steam. **Figure 7(b)**, the t-plot calculates the pore volume and therefore the external pores. **Table 5** shows that the activated hydrochar obtained from the optimum has a specific surface area and micropores surface area of 849.160 and 703.269 $m^2 \cdot g^{-1}$ respectively. This shows that the adsorbent prepared is mainly microporous, and this observation is attributed to the use of steam during the physical activation.

3.4. Adsorption Study of Indigo Carmine

Adsorption isotherms play an important role in the determination of adsorbing capacities and the design of new adsorbents. The effect of the initial concentration of indigo carmine on the adsorption efficiency was studied over the contact time and at a temperature of 22˚C. The quantities adsorbed are calculated experimentally as a function of the equilibrium concentration. The results, corresponding to the variation in the quantity of dye adsorbed at equilibrium on the

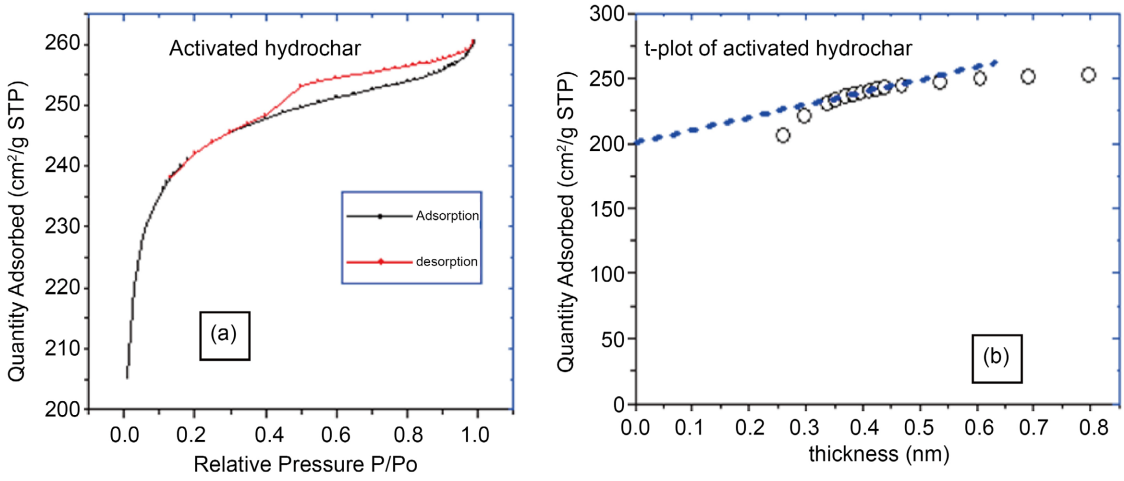

Figure 7. (a) Adsorption-desorption isotherms of N_2 and (b) t-plot for nitrogen adsorbed at 77 K for activated hydrochar obtained at the optimal condition.

Table 5. Textural parameters of the activated hydrochar prepared under optimum condition.

Sample	[a]S_{BET}	[b]S_{mic}	[c]S_{ext}	Total volume	
				[d]V_{mic}	Total volume
AH	849.160	703.269	145.891	0.310	0.402

[q]BET surface area; [b]micropore surface; [c]External surface, [d]micropores volume.

hydrochar as a function of its concentration at equilibrium are shown in **Figure 8**. The plot shows that the adsorption isotherm of indigo carmine on the hydrochar sample is of the L type, characteristic of monolayer adsorption. We note that the quantity adsorbed increases remarkably with the increase in the initial concentration of dye, the quantity adsorbed increases rapidly at the start of the process, followed by gradual saturation of the active sites [21].

The higher the initial concentration (Co), the higher the equilibrium concentration (Ce), indicating relatively strong contact between the active sites of the hydrochar and the indigo carmine molecules. At a certain concentration, the active sites decrease and adsorption also decreases until equilibrium is reached, confirming that it is a monomolecular adsorption with saturation of the monolayer. However, given the characteristics of the activated hydrochar and the size of the indigo carmine, it is possible to predict an accumulation of adsorbate molecules on the surface of the hydrochar in a linear pattern at the mesopore level by the process of capillary condensation. The kinetic study of the elimination of the dye by the prepared adsorbent shows that the quantity of residual concentration decreases as the contact time increases before reaching equilibrium. It should be noted that at the beginning the dye adsorbs on the sites easily accessed, then diffuses to the less accessible sites, and it takes place as stirring time increases until adsorption equilibrium is attained [31].

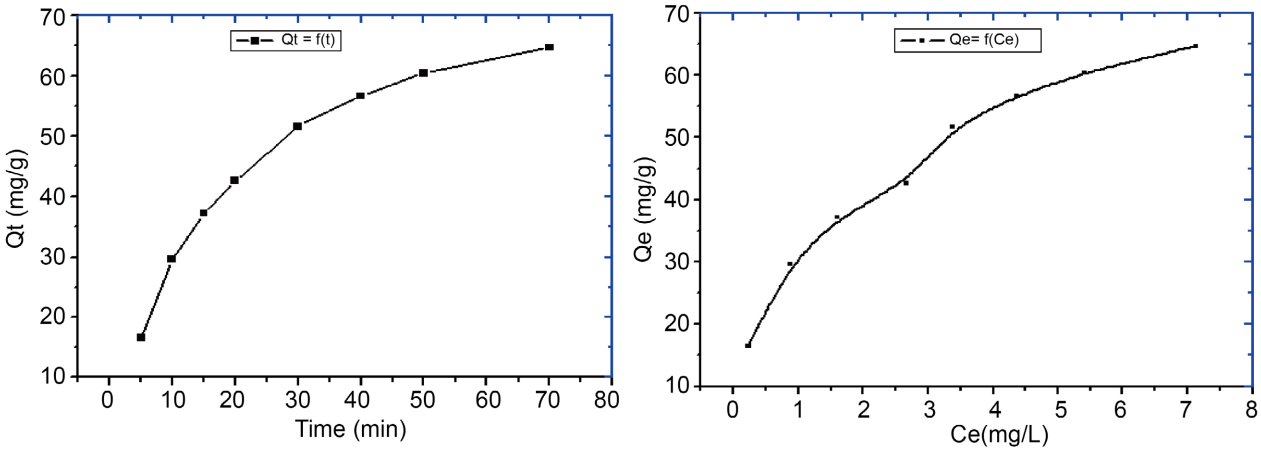

Figure 8. Kinetics and isotherm adsorption of indigo carmine by activated hydrochar.

The equations corresponding to the Freundlich, Langmuir, Temkin and Dubinin-Radushkevich models were applied to the adsorption results (**Figure 9**). The various characteristic adsorption constants for each model were obtained, and all these constants deduced from the linear transformed isotherms are given in **Table 6**.

3.4.1. The Freundlich Isotherm

The linear representation of his equation is expressed as:

$$\log Q_e = \frac{1}{n}\log C_e + \log K_F .$$

This empirical formula has 2 parameters K_F and $\frac{1}{n}$ (Freundlich coefficients), Based on this model, adsorption can only be achieved for the values of $\frac{1}{n}$ ranging between 0.2 and 0.8. In this work, the value of $\frac{1}{n}$ is 0.427 indicating that adsorption is favourable for the retention of the dye on prepared activated hydrochar. In addition, the Freundlich constant K_F equally reflects the adsorption capacity of indigo carmine, the higher the values of K_F, the more the amount of the dye adsorbed will also be. The data in **Table 6** confirm a high level of dye elimination [32].

Langmuir's isotherm advantageously describes phenomena in the form of simple analysis, in a satisfactory manner with weak concentrations and to provide for the existence of an upper limit for stronger concentrations [32]. Plotting the relation $\frac{1}{Q_e}$ with respect to $\frac{1}{C_e}$ has permitted us to calculate the maximum adsorption capacity as well as the adsorption parameters of **Table 6**. The maximum adsorption capacity is Q_m = 128.205 mg/g, reflecting the total coverage of the surface of the adsorbent material by a monolayer. The adsorption constant K_L (0.804 mg/g) is also an indicator of whether or not adsorption is favourable. This value can be explained by the presence of sites favourable to the adsorption of macromolecules on the surface of activated hydrochar.

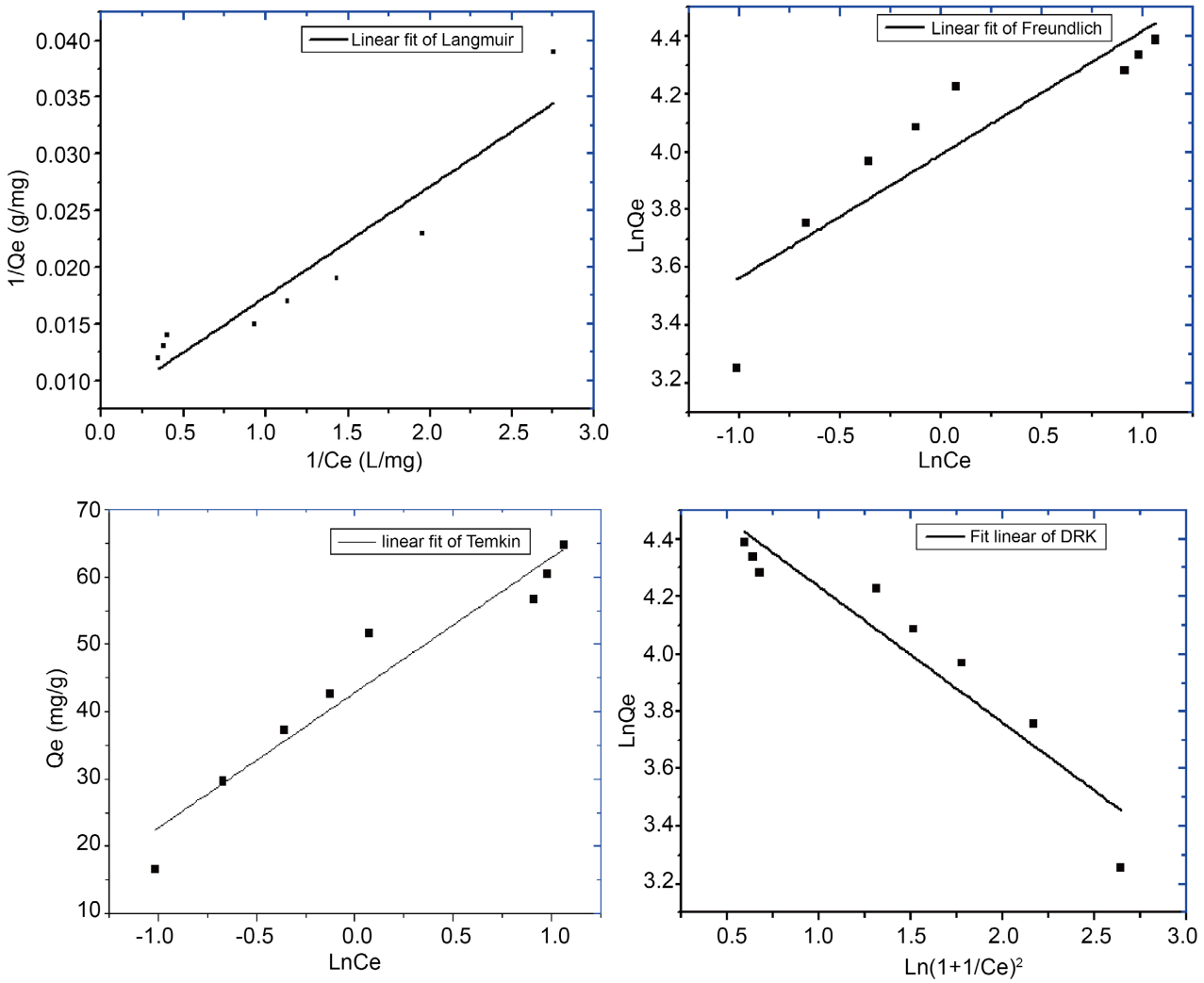

Figure 9. Linear transformed equations of Langmuir; Freundlich, Temkin and Dubinin-Radushkevich model.

Table 6. Isotherm parameters for indigo carmine adsorption using nonlinear and linear regression.

Langmuir			Freundlich		
Q_o (mg/g)	K_L (mL/g)	R^2	1/n	K_F	R^2
128.205	0.804	0.900	0.427	54.163	0.773
TEMKIN			**Dubinin-Radushkevich**		
b_T (J·g/mmol2)	K_T (L/mol)	R^2	K_{DKR} (g^2/J^2)·10^{-9}	Q_{max} (mg/g)	E (J/mol)	R^2
41.4706	380.3088	0.900	47.400	571.748	5.108	0.880

The Temkin model highlights the nature of adsorbent-adsorbate interactions and, as well as the Dubinin-Radushkevich model, provides information on the energetic aspect of adsorption.

The hydrochar sample has a b_T value of around 41.4706 J·g/mmol^2 and therefore indicates that the indigo carmine molecules are attracted to its surface.

The bond equilibrium constant (K_T = 380.3088 L/mol) measures the energy of

the adsorbent-adsorbate bond. The greater the K_T, the stronger the indigo carmine-hydrochar bond and the greater the heat released. Particularly, the correlation coefficient R^2 greater than 0.90 (Table 6), the Temkin model is appropriate for describing the phenomenon of adsorption of dye on these samples by the adsorbent material. According to the Dubinin-Radushkevich model, the energy deduced from the adsorption is equal to 5.108 kJ/mol, characteristic of the Van der Waals-derived forces between the molecules of the indigo carmine and the active sites of the activated hydrochar. As the Dubinin-Radushkevich model is more general, it describes adsorption on a large number of sites (homogeneous and heterogeneous), whereas the Langmuir model only takes homogeneous sites into account. The adsorption capacity of indigo carmine is of the order of 571.748 mg/g, confirming the presence of a mixed porous structure made up of mesopores and micropores.

4. Conclusion

This research work is carried out in two contexts: firstly, it has enabled us to obtain an effective carbonaceous material, based on well-developed operating conditions. In addition, this work enables tannery waste to be recycled by transforming solid waste and then using it to purify liquid tannery waste. The screening of factors allowed us to select three main factors: carbonisation temperature (X_1), residence time (X_2) and moisture content (X_3). These factors were used to obtain responses: hydrochar mass yield (Y_1), iodine value (Y_2) and Methylene Blue value (Y_3), using the Doehlert experimental design methodology. The following optimum preparation conditions were obtained: 83.10%, 390.44 $mg{\cdot}g^{-1}$ and 259.63 $mg{\cdot}g^{-1}$ respectively for hydrochar, iodine and methylene blue indices. The hydrochar is essentially microporous, with a total BET surface area of 849.16 m^2/g and a micropore surface area of 703.269 m^2/g. The IR-FT spectrum shows hydroxyl groups O-H; C-H; C-N and C-O. The corresponding adsorption isotherms show that hydrochar better adsorbs the dyes in an aqueous solution with a good adsorption capacity. The prepared Hydrochar demonstrates higher capacities of adsorption than that which are currently used for environmental remediation. The value of surface area and micropore quantity indicated that the prepared adsorbent can be used in medicine for food disintoxication. Furthermore, the variety of functions present at the surface implies that the prepared Hydrochar can be used as catalysts and catalyst supports.

Acknowledgements

Authors gratefully acknowledge the technical support of the Laboratory of Applied Organic Chemistry, Analysis and Environmental Unit, Faculty of Science Semlalia, University Caddy Ayyad of Marrakech in Morocco.

Conflicts of Interest

The authors declare no conflicts of interest regarding the publication of this paper.

References

[1] Bamberger, Y. and Rogeaux, B. (2007) Quelles solutions des industriels peuvent-ils apporter aux problèmes énergétiques? *Revue de l Energie*, **575**, 5-16.

[2] REN21. Renewables (2013) Global Status Report. Technical Report.

[3] Mochidzuki, K., Sato, N. and Sakoda, A. (2005) Production and Characterization of Carbonaceous Adsorbents from Biomass Wastes by Aqueous Phase Carbonization. *Adsorption*, **11**, 669-673. https://doi.org/10.1007/s10450-005-6004-6

[4] Jjagwe, J., Olupot, P.W., Menya, E. and Kalibbala, H.M. (2021) Synthesis and Application of Granular Activated Carbon from Biomass Waste Materials for Water Treatment: A Review. *Journal of Bioresources and Bioproducts*, **6**, 292-322. https://doi.org/10.1016/j.jobab.2021.03.003

[5] Tang, Z., Lim, S., Pang, Y., Shuit, S. and Ong, H. (2020) Utilisation of Biomass Wastes Based Activated Carbon Supported Heterogeneous Acid Catalyst for Biodiesel Production. *Renewable Energy*, **158**, 91-102. https://doi.org/10.1016/j.renene.2020.05.119

[6] Sun, Y., Li, H., Li, G., Gao, B., Yue, Q. and Li, X. (2016) Characterization and Ciprofloxacin Adsorption Properties of Activated Carbons Prepared from Biomass Wastes by H_3PO_4 Activation. *Bioresource Technology*, **217**, 239-244. https://doi.org/10.1016/j.biortech.2016.03.047

[7] Cavali, M., Libardi Junior, N., de Sena, J.D., Woiciechowski, A.L., Soccol, C.R., Belli Filho, P., *et al*. (2023) A Review on Hydrothermal Carbonization of Potential Biomass Wastes, Characterization and Environmental Applications of Hydrochar, and Biorefinery Perspectives of the Process. *Science of the Total Environment*, **857**, Article 159627. https://doi.org/10.1016/j.scitotenv.2022.159627

[8] Jain, A., Balasubramanian, R. and Srinivasan, M.P. (2016) Hydrothermal Conversion of Biomass Waste to Activated Carbon with High Porosity: A Review. *Chemical Engineering Journal*, **283**, 789-805. https://doi.org/10.1016/j.cej.2015.08.014

[9] Funke, A. and Ziegler, F. (2010) Hydrothermal Carbonization of Biomass: A Summary and Discussion of Chemical Mechanisms for Process Engineering. *Biofuels, Bioproducts and Biorefining*, **4**, 160-177. https://doi.org/10.1002/bbb.198

[10] Oliveira, I., Blöhse, D. and Ramke, H. (2013) Hydrothermal Carbonization of Agricultural Residues. *Bioresource Technology*, **142**, 138-146. https://doi.org/10.1016/j.biortech.2013.04.125

[11] Maniscalco, M.P., Volpe, M. and Messineo, A. (2020) Hydrothermal Carbonization as a Valuable Tool for Energy and Environmental Applications: A Review. *Energies*, **13**, Article 4098. https://doi.org/10.3390/en13164098

[12] Titirici, M., Thomas, A. and Antonietti, M. (2007) Back in the Black: Hydrothermal Carbonization of Plant Material as an Efficient Chemical Process to Treat the CO_2 Problem? *New Journal of Chemistry*, **31**, 787-789. https://doi.org/10.1039/b616045j

[13] Hoekman, S.K., Broch, A. and Robbins, C. (2011) Hydrothermal Carbonization (HTC) of Lignocellulosic Biomass. *Energy & Fuels*, **25**, 1802-1810. https://doi.org/10.1021/ef101745n

[14] Sugimoto, Y., Miki, Y., Hayamizu, K., Umeda, S., Komano, T., Mashimo, K., *et al*. (1996) Characterization of Thermally Decomposed Cellulose and Red Pine at 200˚C in Water. *Journal of the Japan Institute of Energy*, **75**, 829-838. https://doi.org/10.3775/jie.75.829

[15] Masoumi, S., Borugadda, V.B., Nanda, S. and Dalai, A.K. (2021) Hydrochar: A Review on Its Production Technologies and Applications. *Catalysts*, **11**, Article 939.

https://doi.org/10.3390/catal11080939

[16] Aragón-Briceño, C.I., Pozarlik, A.K., Bramer, E.A., Niedzwiecki, L., Pawlak-Kruczek, H. and Brem, G. (2021) Hydrothermal Carbonization of Wet Biomass from Nitrogen and Phosphorus Approach: A Review. *Renewable Energy*, **171**, 401-415. https://doi.org/10.1016/j.renene.2021.02.109

[17] Nana, L.A (2012). Etude et réalisation des opérations de rivière: Cas de la tannerie moderne de la Bénoué. Rapport de stage de fin d'études en vue de l'obtention du diplôme d'ingénieur de travaux en technologie du textile. ISS Université de Maroua.

[18] Mendondjio, L.L. (2012) La peau fraiche: De son origine a sa commercialisation avant le tannage. Rapport de stage de fin d'étude en vue de l'obtention du diplôme d'ingénieur de travaux en technologie du textile. ISS Université de Maroua.

[19] Park, D., Yun, Y., Hye Jo, J. and Park, J.M. (2005) Mechanism of Hexavalent Chromium Removal by Dead Fungal Biomass of Aspergillus Niger. *Water Research*, **39**, 533-540. https://doi.org/10.1016/j.watres.2004.11.002

[20] Louarrat, M. (2017) Removal of Chromium Cr(Vi) of Tanning Effluent with Activated Carbon from Tannery Solid Wastes. *American Journal of Physical Chemistry*, **6**, 103-109. https://doi.org/10.11648/j.ajpc.20170606.11

[21] Debina, B., Baçaoui, A., Tamafo Fouégué, A.D., Kouotou, D., Rahman, A.N., Yaacoubi, A., *et al*. (2023) Hydrothermal Carbonization of Vegetable-Tanned Leather Shavings (HTC-VTS) for Environmental Remediation: Optimization of Process Conditions. *Royal Society Open Science*, **10**, Article 230302. https://doi.org/10.1098/rsos.230302

[22] Jais, F.M., Chee, C.Y., Ismail, Z. and Ibrahim, S. (2021) Experimental Design via Naoh Activation Process and Statistical Analysis for Activated Sugarcane Bagasse Hydrochar for Removal of Dye and Antibiotic. *Journal of Environmental Chemical Engineering*, **9**, Article 104829. https://doi.org/10.1016/j.jece.2020.104829

[23] Lekene, R.B.N., Ankoro, N.O., Nsami, N.J., Kouotou, D., Rahman, A.N. and Mbadacam, K.J. (2020) Preparation of Activated Carbons Based Balanites Aegyptiaca Shells by Chemical Activation: Optimization Conditions Using the Methodology of Experimental Design. *European Journal of Advanced Chemistry Research*, **1**, 1-7. https://doi.org/10.24018/ejchem.2020.1.6.33

[24] Rabier, F. (2007) Modélisation par la méthode des plans d'expériences du comportement dynamique d'un module IGBT utilisé en traction ferroviaire. Thèse. Institut nationale polytechnique de Toulouse.

[25] Goupy, J. (2006) Les plans d'expériences. Revue MODULAD, No. 34, 74-116.

[26] Goupy, J. and Creighton, L. (2006) Introduction aux plans d'expériences. 3ème édition, Dunod, 325.

[27] Kouotou, D., Manga, H.N., Baçaoui, A., Yaacoubi, A. and Mbadcam, J.K. (2013) Optimization of Activated Carbons Prepared by H_3PO_4 and Steam Activation of Oil Palm Shells. *Journal of Chemistry*, **2013**, Article 654343. https://doi.org/10.1155/2013/654343

[28] Kwaghger, A. and Ibrahim, J. (2013) Optimization of Conditions for the Preparation of Activated Carbon from Mango Nuts Using HCl. *American Journal of Engineering Research and Reviews*, **2**, 74-85.

[29] Enaime, G., Baçaoui, A., Yaacoubi, A., Wichern, M. and Lübken, M. (2020) Hydrothermal Carbonization of the Filter Bed Remained After Filtration of Olive Mill Wastewater on Olive Stones for Biofuel Application. *Biomass Conversion and Biorefinery*, **12**, 1237-1247. https://doi.org/10.1007/s13399-020-00743-9

[30] Bedin, K.C., Cazetta, A.L., Souza, I.P.A.F., Pezoti, O., Souza, L.S., Souza, P.S.C., *et al*. (2018) Porosity Enhancement of Spherical Activated Carbon: Influence and Optimization of Hydrothermal Synthesis Conditions Using Response Surface Methodology. *Journal of Environmental Chemical Engineering*, **6**, 991-999. https://doi.org/10.1016/j.jece.2017.12.069

[31] Ndi Nsami, J. and Ketcha Mbadcam, J. (2013) The Adsorption Efficiency of Chemically Prepared Activated Carbon from Cola Nut Shells by on Methylene Blue. *Journal of Chemistry*, **2013**, Article 469170. https://doi.org/10.1155/2013/469170

[32] Debina, B., Eric, S.N., Fotio, D., Arnaud, K.T., Lemankreo, D. and Rahman, A.N. (2020) Adsorption of Indigo Carmine Dye by Composite Activated Carbons Prepared from Plastic Waste (PET) and Banana Pseudo Stem. *Journal of Materials Science and Chemical Engineering*, **8**, 39-55. https://doi.org/10.4236/msce.2020.812004